

Excitonic effects on the two-color coherent control of interband transitions in bulk semiconductors

R. D. R. Bhat and J. E. Sipe

*Department of Physics and Institute for Optical Sciences,
University of Toronto, 60 St. George Street,
Toronto, Ontario M5S 1A7, Canada*

(Dated: March 23, 2022)

Abstract

Quantum interference between one- and two-photon absorption pathways allows coherent control of interband transitions in unbiased bulk semiconductors; carrier population, carrier spin polarization, photocurrent injection, and spin current injection may all be controlled. We extend the theory of these processes to include the electron-hole interaction. Our focus is on photon energies that excite carriers above the band edge, but close enough to it so that transition amplitudes based on low order expansions in \mathbf{k} are applicable; both allowed-allowed and allowed-forbidden two-photon transition amplitudes are included. Analytic solutions are obtained using the effective mass theory of Wannier excitons; degenerate bands are accounted for, but envelope-hole coupling is neglected. We find a Coulomb enhancement of two-color coherent control process, and relate it to the Coulomb enhancements of one- and two-photon absorption. In addition, we find a frequency dependent phase shift in the dependence of photocurrent and spin current on the optical phases. The phase shift decreases monotonically from $\pi/2$ at the band edge to 0 over an energy range governed by the exciton binding energy. It is the difference between the partial wave phase shifts of the electron-hole envelope function reached by one- and two-photon pathways.

I. INTRODUCTION

The phenomenon of quantum interference can be used to control physical and chemical processes. One approach, the ‘ $n + m$ ’ scheme, uses a two-color light field to interfere n - and m -photon transitions.^{1,2,3} Interference between one- and two-photon transitions, for example, allows controllable polar asymmetry of photoelectrons in atomic ionization,^{4,5} controllable dissociation of HD^+ ,⁶ and controllable photocurrent injection in unbiased solids due to free carrier absorption,⁷ impurity-band transitions,⁸ and quantum well bound-continuum intersubband transitions.⁹ In biased asymmetric semiconductor double wells, ‘ $1 + 2$ ’ interference allows control of carrier population and THz emission.¹⁰ Interband ‘ $1 + 2$ ’ interference in unbiased semiconductors, which is our interest here, allows independent control of electrical current injection^{11,12} and spin current injection.^{13,14,15,16,17,18} Furthermore, in non-centrosymmetric semiconductors, it allows independent control of carrier populations (i.e., absorption)^{19,20} and carrier spin polarization.^{21,22} In each scenario, the experimenter can control the interference by adjusting the phases of the two colors.

The controllable optical phases are not the only source of phase between the transition amplitudes. In general, there is also a material-dependent intrinsic phase.²³ Phenomenologically, the intrinsic phase appears as a phase shift in the dependence of the process on a relative phase parameter of the optical fields. Additionally, selectivity between two processes is possible when their intrinsic phases differ²⁴; for example, ‘ $1+3$ ’ experiments on diatomic molecules have controlled the branching ratio of ionization and dissociation channels.²⁵ The intrinsic phase can be strongly frequency dependent near resonances,²⁵ and the hope that it might serve as a new spectroscopic observable^{26,27} has led to efforts to understand its physical origin.

Whereas a resonance is necessary for a phase shift to a ‘ $1+3$ ’ process,²⁶ it is not necessary for a phase shift to a ‘ $1+2$ ’ process. For example, an intrinsic phase in the ‘ $1+2$ ’ photoionization of atoms is predicted from the simple model of a delta function potential.^{28,29}

Nevertheless, microscopic theories for the interband ‘ $1 + 2$ ’ processes in bulk semiconductors have until now predicted trivial intrinsic phases.^{11,13,19,21} The photocurrent, for example, was predicted to be proportional to the sine of the relative phase parameter for all final energies.¹¹ Each of these theories use the independent particle approximation, in which the Coulomb attraction between the injected electron and hole is neglected. That approxima-

tion is expected to be good for final energies well above the band gap, since in this case the electron and hole travel quickly away from each other. However, close to the band gap, one generally expects to see deviations from the independent particle approximation. In the one-photon absorption spectrum, for instance, it is well known that the electron-hole attraction is responsible for exciton lines below the band gap, and for an enhancement of the absorption above the gap known as *Sommerfeld* or *Coulomb enhancement*.³⁰

The effect of the electron-hole attraction on one-photon absorption has been studied with various degrees of sophistication. On the one hand, modern *ab initio* calculations that include Coulomb effects have recently given very good quantitative agreement with experimental spectra,^{31,32,33,34,35} although at the cost of significant computational overhead. On the other hand, simple models of Wannier excitons can describe Coulomb effects near the band edge of many direct gap semiconductors. These excitonic effects have long been understood qualitatively on the basis of a simple two-band model in the effective mass approximation,³⁶ which is even quantitatively accurate for typical semiconductors.³⁴

Excitonic effects on nonlinear optical properties of bulk semiconductors have also been studied in the effective mass, Wannier exciton approximation^{37,38,39,40,41,42,43,44,45,46,47,48,49,50} and only recently with *ab initio* methods.⁵¹ The two-photon absorption spectrum shows a different set of exciton lines and a Coulomb enhancement that is weaker than its one-photon counterpart.

One- and two-photon absorption spectra have been measured sufficiently often that excitonic effects on them are well established. In contrast, semiconductor ‘1+2’ interference experiments have been done typically at only a single energy and typically many exciton binding energies above the band-gap. Moreover, these initial experiments lacked an absolute calibration of the relative optical phase, and thus were insensitive to the intrinsic phase. Such a calibration is possible,⁵² and could be used to verify the predictions we present here. A nontrivial intrinsic phase would have implications for the use of ‘1+2’ current injection as an absolute measurement of the carrier-envelope phase of an ultrashort optical pulse.^{53,54,55}

In the present work, we extend the theory of ‘1+2’ coherent control of bulk semiconductor interband transitions beyond the independent particle approximation, employing a set of approximations that are valid close to the Γ point of a direct gap bulk semiconductor. Our investigation is limited to a perturbative treatment in the fields. In this limit of low photoinjected carrier density, the only inter-particle interaction of importance is that between

a single electron and hole. We show that, due to the electron-hole attraction, a nontrivial phase shift does in fact occur in the control of current and spin current, but not in the control of carrier population or spin polarization. The intrinsic phase can be understood in terms of partial wave phase shifts due to the Coulomb potential between electron and hole. In addition, we find an enhancement of each process, and relate it to the Coulomb enhancements of one- and two-photon absorption.

In the next section, we establish notation necessary to describe the ‘1+2’ processes in terms of one- and two-photon transition amplitudes. In section III, we present the microscopic model. The transition amplitudes are worked out in section IV. The final expressions for the ‘1+2’ effects are given in section V, and numerical results for GaAs are presented. In section VI, further understanding of the enhancement and intrinsic phase is discussed, and we examine the ratios often used as figures of merit for ‘1+2’ effects. Intermediate state Coulomb enhancement is examined in Appendix A. For reference, the current injection tensor is worked out for parabolic bands in Appendix B.

II. PRELIMINARIES

The rate of photocurrent injection into an unbiased bulk semiconductor by a two color light field $\mathbf{E}(t) = \mathbf{E}_\omega \exp(-i\omega t) + \mathbf{E}_{2\omega} \exp(-i2\omega t) + c.c.$ can be written

$$\frac{dJ^i}{dt} = \eta_{(I)}^{ijkl} E_\omega^{*j} E_\omega^{*k} E_{2\omega}^l + c.c., \quad (1)$$

where superscripts denote Cartesian components and repeated indices are to be summed over.¹¹ The fourth rank tensor $\eta_{(I)}$, called the current injection tensor, describes the material response. It is purely imaginary in the independent particle approximation,¹¹ but can be complex in general. We define the intrinsic phase δ^{ijkl} of the component $\eta_{(I)}^{ijkl}$ as

$$\delta^{ijkl} = \arctan \left(\text{Re} \left(\eta_{(I)}^{ijkl} \right) / \text{Im} \left(\eta_{(I)}^{ijkl} \right) \right) \quad (2)$$

so that it is zero or π in the independent particle approximation. When the electron-hole interaction is included in the set of approximations used below, all the components of $\eta_{(I)}$ have the same phase. That is,

$$\eta_{(I)}^{ijkl} = i e^{i\delta} \left| \eta_{(I)}^{ijkl} \right|. \quad (3)$$

The intrinsic phase δ appears as a phase shift in the dependence of the current injection on the phase of the optical fields. For co-linearly polarized fields ($\mathbf{E}_\omega = E_\omega \exp(i\phi_\omega)\hat{\mathbf{x}}$ and $\mathbf{E}_{2\omega} = E_{2\omega} \exp(i\phi_{2\omega})\hat{\mathbf{x}}$), for example, the current injection is

$$\frac{d\mathbf{J}}{dt} = 2E_\omega^2 E_{2\omega} |\eta_{(I)}^{xxxx}| \sin(2\phi_\omega - \phi_{2\omega} - \delta) \hat{\mathbf{x}}.$$

We are ignoring scattering processes through which the current would relax to a steady state value under continuous illumination, or would decay to zero following pulsed excitation. The current injection discussed here can be used as a source term in hydrodynamic equations that treat the scattering phenomenologically^{11,56,57} or in microscopic transport equations.⁵⁸ Coulomb effects other than the excitonic effects we consider here play a role in scattering, especially at high densities of excited carriers. Such Coulomb effects are outside the scope of this paper.

The current injection tensor can be written in terms of one- and two-photon transition amplitudes. We take as the initial state a clean, cold semiconductor. In a Fermi's golden rule calculation for the ballistic current, light produces transitions to final states $|n\rangle$ with velocity \mathbf{v}_{nn} , probability amplitude c_n , and energy $\hbar\omega_n$ above the ground state. The final states will be specified in detail in the next section; here the label n represents the set of quantum numbers for either an interacting or independent electron-hole pair. Thus,

$$\begin{aligned} \frac{d}{dt}\mathbf{J} &= \frac{e}{L^3} \sum_n \mathbf{v}_{nn} \frac{d}{dt} |c_n|^2 \\ &= \frac{2\pi e}{L^3} \sum_n \mathbf{v}_{nn} |\Omega_n^{(1)} + \Omega_n^{(2)}|^2 \delta(2\omega - \omega_n) \\ &= \frac{2\pi e}{L^3} \sum_n \mathbf{v}_{nn} \left\{ |\Omega_n^{(1)}|^2 + |\Omega_n^{(2)}|^2 + (\Omega_n^{(1)} \Omega_n^{(2)*} + c.c.) \right\} \delta(2\omega - \omega_n), \end{aligned} \tag{4}$$

where e is the electron charge (negative), L^3 is a normalization volume, and $\Omega_n^{(i)}$ is the amplitude for an i -photon transition. The $\Omega_n^{(i)}$ take the form

$$\Omega_n^{(1)} = \mathbf{E}_{2\omega} \cdot \mathbf{D}_n^{(1)} \tag{5}$$

$$\Omega_n^{(2)} = \mathbf{E}_\omega \mathbf{E}_\omega : \mathbf{D}_n^{(2)}, \tag{6}$$

where the vector $\mathbf{D}_n^{(1)}$ and second rank tensor $\mathbf{D}_n^{(2)}$ depend only on properties of the material. We consider them in detail in section IV.

In the last equation of (4), the first term is (one-photon) one-color current injection, the second term describes two-photon one-color current injection, while the interference term

describes the ‘1+2’ current. Because of their different dependencies on the electric field amplitudes, these three terms can in principle be separated experimentally. But the first two terms vanish for centrosymmetric crystals, and the first vanishes even for zincblende crystals; we neglect them here. Excitonic effects on the first term were studied by Shelest and Éntin.^{59,60} The third term survives in all materials. Comparing its expression with the phenomenological form (1), we have

$$\eta_{(I)}^{ijkl} = \frac{2\pi e}{L^3} \sum_n v_{nn}^i (D_n^{(2)*})^{jk} (D_n^{(1)})^l \delta(2\omega - \omega_n). \quad (7)$$

Even if scattering from impurities and phonons is neglected, the injection current described by (4) does not capture the full current density; there are also optical rectification and ‘shift’ contributions to the current.⁶¹ The one-color varieties of these have been studied in some detail,^{60,62,63,64} but the ‘1+2’ varieties have not. However, the different time dependencies of the three current contributions allows for their separate examination experimentally, at least in principle, and rough order-of-magnitude estimates indicate that typically the injection current will be the largest; it is the only contribution to the current we treat here.

As in (4), the carrier injection rate can be written as

$$\begin{aligned} \frac{d}{dt}n &= \frac{1}{L^3} \sum_n \frac{d}{dt} |c_n|^2 \\ &= \frac{2\pi}{L^3} \sum_n \left\{ |\Omega_n^{(1)}|^2 + |\Omega_n^{(2)}|^2 + (\Omega_n^{(1)} \Omega_n^{(2)*} + c.c.) \right\} \delta(2\omega - \omega_n), \end{aligned} \quad (8)$$

where n is the number density of injected electron-hole pairs. The first two terms in (8) are the usual one- and two-photon absorption rates, which we denote by $\dot{n}_{2\omega}$ and \dot{n}_ω respectively. In terms of one- and two-photon coefficients $\xi_{(1)}^{ij}$ and $\xi_{(2)}^{ijkl}$ that depend only on the properties of the material, they can be written as $\dot{n}_{2\omega} = \xi_{(1)}^{ij} E_{2\omega}^i E_{2\omega}^{*j}$ and $\dot{n}_\omega = \xi_{(2)}^{ijkl} E_\omega^i E_\omega^j E_\omega^{*k} E_\omega^{*l}$.¹¹ From (8),

$$\xi_{(1)}^{ij} = \frac{2\pi}{L^3} \sum_n (D_n^{(1)*})^i (D_n^{(1)})^j \delta(2\omega - \omega_n) \quad (9)$$

$$\xi_{(2)}^{ijkl} = \frac{2\pi}{L^3} \sum_n (D_n^{(2)*})^{ij} (D_n^{(2)})^{kl} \delta(2\omega - \omega_n). \quad (10)$$

The third term in (8), denoted \dot{n}_I , allows population control as discussed and observed by Fraser *et al.*^{19,20} It can be written in terms of a third rank tensor $\xi_{(I)}^{ijk}$ as¹⁹

$$\dot{n}_I = \xi_{(I)}^{ijk} E_\omega^{*i} E_\omega^{*j} E_{2\omega}^k + c.c., \quad (11)$$

where

$$\xi_{(I)}^{ijk} = \frac{2\pi}{L^3} \sum_n (D_n^{(2)*})^{ij} (D_n^{(1)})^k \delta(2\omega - \omega_n). \quad (12)$$

It is purely real in the independent particle approximation.^{19,20}

Expressions such as (4) and (8) can also be written for carrier spin polarization and spin current.²² The interference terms of these describe ‘1+2’ spin control²¹ and ‘1+2’ spin current injection,¹³ which can be written in terms of material response pseudotensors $\zeta_{(I)}^{ijkl21}$ and $\mu_{(I)}^{ijklm}$,¹⁷ respectively. In the independent particle approximation, $\zeta_{(I)}^{ijkl}$ is purely imaginary,²¹ while $\mu_{(I)}^{ijklm}$ is purely real.¹⁷

The phases of the material response tensors $\eta_{(I)}$, $\xi_{(I)}$, $\mu_{(I)}$, and $\zeta_{(I)}$ are related to the phases of the one- and two-photon matrix elements, $\mathbf{D}_n^{(1)}$ and $\mathbf{D}_n^{(2)}$. The one- and two-photon matrix elements also appear, respectively, in the one- and two-photon absorption coefficients, as can be seen from (9) and (10). There have been many theoretical investigations of one- and two-photon absorption near the direct gap of bulk semiconductors that include excitonic effects.^{65,66} However, since one- and two-photon absorption are insensitive to the phases of the transition amplitudes, those calculations took no care to get the phases of the transition amplitudes correct. In the next two sections we find the transition amplitudes with the correct phases including excitonic effects.

III. MODEL

We first review the two-band effective mass model of Wannier excitons; the two bands are nondegenerate conduction and valence bands that are parabolic and isotropic with a direct gap E_{cv}^g at $\mathbf{k} = \mathbf{0}$ (the Γ point).^{67,68} It has been used to study excitonic effects on one-photon absorption,³⁶ two-photon absorption,³⁸ and other nonlinear optical processes.^{44,45,46,47,48,49,50} We subsequently describe a generalization that accounts for degeneracy and multiple bands. It has been used for two-photon absorption,⁴⁰ and has been implied whenever two-band results have been applied to actual semiconductors.

The total Hamiltonian of the system can be written in the form $H = H_B + H_C + H_{\text{int}}(t)$. Here, $H_0 = H_B + H_C$ is the field-free Hamiltonian made up of the single-particle part H_B and the part due to the Coulomb interaction between carriers H_C . Using the minimal coupling Hamiltonian, the optical perturbation takes the form $H_{\text{int}}(t) = -(e/c) \mathbf{A}(t) \cdot \mathbf{v} + e^2 A^2 / (2mc^2)$, where $\mathbf{A}(t)$ is the vector potential associated with the Maxwell electric field and \mathbf{v} is the

velocity operator associated with H_0 . In the long wavelength limit, the position dependence of $\mathbf{A}(t)$ is neglected, and thus the second term in $H_{\text{int}}(t)$ may be neglected, since it can simply be absorbed in an overall time-dependent phase of the full system ket and hence cannot cause any transitions between states of H_0 . Many approximate approaches to band structure calculation, including most pseudopotentials, and the truncation to a finite number of bands, implicitly assume an underlying field-free Hamiltonian that is nonlocal; there is then a correction to the interaction Hamiltonian $H_{\text{int}}(t)$ in the velocity gauge.^{43,69} However, we neglect such nonlocal corrections, as has been the practice in previous calculations of coherent control effects.^{11,13,19}

The initial state is the “vacuum” $|0\rangle$; it corresponds to completely filled valence bands and empty conduction bands. If the Coulomb interaction were neglected in a two-band model consisting of valence (v) and conduction (c) bands, the final states would be of the form $a_{c\mathbf{k}}^\dagger a_{v\mathbf{k}} |0\rangle$, where the operator $a_{n\mathbf{k}}^\dagger$ creates an electron in an eigenstate of H_B , a Bloch state $|n, \mathbf{k}\rangle$ with band index n and wavevector \mathbf{k} . The photon momentum has been neglected, consistent with the long wavelength approximation. The Coulomb interaction couples states at different \mathbf{k} ; thus including H_C the final states are of the form

$$|cv\boldsymbol{\kappa}\rangle \equiv \sum_{\mathbf{k}} A_{cv}^{\boldsymbol{\kappa}}(\mathbf{k}) a_{c\mathbf{k}}^\dagger a_{v\mathbf{k}} |0\rangle, \quad (13)$$

where $\boldsymbol{\kappa}$ labels the state; its physical meaning is given below. In the effective mass Wannier exciton approximation, the Fourier transform

$$\psi_{cv}^{\boldsymbol{\kappa}}(\mathbf{r}) = \sum_{\mathbf{k}} A_{cv}^{\boldsymbol{\kappa}}(\mathbf{k}) e^{i\mathbf{k}\cdot\mathbf{r}}, \quad (14)$$

which is the wavefunction for the relative coordinate between electron and hole, is a hydrogenic wavefunction satisfying

$$-\frac{\hbar^2}{2\mu_{cv}} \nabla^2 \psi_{cv}^{\boldsymbol{\kappa}}(\mathbf{r}) - V(r) \psi_{cv}^{\boldsymbol{\kappa}}(\mathbf{r}) = (E_{cv}(\boldsymbol{\kappa}) - E_{cv}^g) \psi_{cv}^{\boldsymbol{\kappa}}(\mathbf{r}), \quad (15)$$

where $\mu_{cv}^{-1} = m_c^{-1} + m_v^{-1}$ is the reduced mass in terms of the (positive) conduction and valence band effective masses, and $V(r)$ is the Coulomb potential, $V(r) = e^2/(\epsilon r)$, screened by the static dielectric constant ϵ .^{30,36,70} The state has energy

$$E_{cv}(\boldsymbol{\kappa}) = \frac{\hbar^2 \kappa^2}{2\mu_{cv}} + E_{cv}^g.$$

We choose the states to be normalized over the volume L^3 by $\langle m, \mathbf{k} | n, \mathbf{k} \rangle = \delta_{n,m} \delta_{\mathbf{k}, \mathbf{k}'}$ and $\langle cv\boldsymbol{\kappa} | cv\boldsymbol{\kappa}' \rangle = \delta_{\boldsymbol{\kappa}, \boldsymbol{\kappa}'}$; as a result $\psi_{cv}^{\boldsymbol{\kappa}}(\mathbf{r})$ is unitless, having the normalization $\int d^3r (\psi_{cv}^{\boldsymbol{\kappa}}(\mathbf{r}))^* \psi_{cv}^{\boldsymbol{\kappa}'}(\mathbf{r}) = L^3 \delta_{\boldsymbol{\kappa}, \boldsymbol{\kappa}'}$.

Our focus in this paper is on the unbound solutions to (15); bound exciton states lack relative velocity between the electron and hole, and hence do not contribute to the ballistic current or spin current. For a Fermi's golden rule calculation of the current or spin current, the unbound state must behave asymptotically like an outgoing plane wave in the relative coordinate between electron and hole; $\boldsymbol{\kappa}$ is the wavevector of the outgoing plane wave. Specifically, we must use “ionization states” rather than scattering states,⁷¹ as was done for atomic ‘1+2’ ionization.²⁸ They are related by $(\psi_{cv}^{\boldsymbol{\kappa}}(\mathbf{r}))_{\text{ion}} = [(\psi_{cv}^{-\boldsymbol{\kappa}}(\mathbf{r}))_{\text{scatt}}]^*$.⁷² Calculations of one- or two-photon absorption are insensitive to an error in this choice of boundary condition, but the present calculation is not, since it is sensitive to the relative phase of the transition amplitudes.

The ionization state wavefunctions that solve (15) can be expressed as a sum over partial waves,

$$\psi_{cv}^{\boldsymbol{\kappa}}(\mathbf{r}) = e^{\frac{\pi}{2a_{cv}\kappa}} \sum_{l=0}^{\infty} \frac{\Gamma\left(l+1+\frac{i}{a_{cv}\kappa}\right)}{(2l)!} (2i\kappa r)^l e^{-i\kappa r} P_l\left(\frac{\mathbf{r} \cdot \boldsymbol{\kappa}}{r\kappa}\right) {}_1F_1\left(l+1+\frac{i}{a_{cv}\kappa}; 2l+2; 2i\kappa r\right), \quad (16)$$

where $a_{cv} = \epsilon \hbar^2 / (\mu_{cv} e^2)$ is the exciton Bohr radius, and κ and r mean $|\boldsymbol{\kappa}|$ and $|\mathbf{r}|$.⁷³ The P_l are Legendre polynomials, ${}_1F_1$ is a confluent hypergeometric function, and Γ is the Gamma function.

Such a two-band model of Wannier excitons is useful for the description of many optical properties. However, near the band gap at the Γ point of a typical zincblende semiconductor there are, counting spin, eight bands: two each of conduction (c), heavy hole (hh), light hole (lh) and split-off hole (so). Other bands, especially the next higher conduction bands, can also be important for some processes, especially for population and spin control.

The existence of multiple bands and band degeneracy modifies the exciton Hamiltonian, i.e., the operator acting on $\psi_{cv}^{\boldsymbol{\kappa}}(\mathbf{r})$ in the left side of (15). In the effective mass approximation, using a basis of Γ point states, the kinetic part of the Wannier exciton Hamiltonian has a matrix structure.^{75,76} Even though this approximation neglects band warping, non-parabolicity, and inversion asymmetry, the Hamiltonian lacks analytic eigenstates.⁷⁶ This is essentially due to the degeneracy of the hh and lh bands at the Γ point. As a result of the

difference between m_{hh} and m_{lh} there is ‘envelope-hole coupling’,⁷⁷ which is a spin-orbit-like coupling between the orbital angular momentum of the exciton envelope function and the total angular momentum of the valence band Γ point Bloch functions.⁷⁸ Baldereschi and Lipari split the effective mass Hamiltonian into a sum of terms based on symmetry, and showed that in a spherical approximation the envelope-hole coupling could be treated as a perturbation to the diagonal part, which has analytic, hydrogenic eigenstates.^{70,79} In order to extract the main physics, while preserving the simplicity of the two-band model, we neglect envelope-hole coupling entirely. In this approximation, (15) remains valid for each conduction-valence band pair, however one must use ‘average’ effective masses for degenerate bands. Specifically, the effective mass of the valence bands hh , lh , and so is m/γ_{1L} , where m is the free electron mass, and γ_{1L} is one of the Luttinger parameters.⁷⁰ The upper conduction bands have a different average effective mass. Note that $\psi_{cv}^{\kappa}(\mathbf{r})$ is independent of c and v within the set of bands $\{c, hh, lh, so\}$. The effect of envelope-hole coupling has been studied for exciton bound states,^{42,70,79} but not for optical processes involving unbound excitons in the continuum.

Even within this model, the presence of multiple bands provides two types of terms in the sum over intermediate states in the two-photon amplitude: two-band terms, in which the intermediate and final states are in the same exciton series [i.e., two states of the form (13) with the same c and v], and three-band terms, in which the intermediate and final states are in different series. Three-band terms are important for some processes but not for others. For current control, three-band terms are important for cross-linearly polarized fields,⁸⁰ and for spin current control, they are important for the spin current due to co-linearly polarized fields.¹³ Three-band terms are essential for population and spin control.^{22,80}

The velocity matrix elements involving the state $|cv\kappa\rangle$ are

$$\langle cv\kappa | \mathbf{v} | 0 \rangle = \sum_{\mathbf{k}} (A_{cv}^{\kappa}(\mathbf{k}))^* \mathbf{v}_{cv}(\mathbf{k}) \quad (17)$$

$$\langle cv\kappa | \mathbf{v} | c'v'\kappa' \rangle = \sum_{\mathbf{k}} (A_{cv}^{\kappa}(\mathbf{k}))^* A_{c'v'}^{\kappa'}(\mathbf{k}) (\mathbf{v}_{cc'}(\mathbf{k}) \delta_{v,v'} - \mathbf{v}_{v'v}(\mathbf{k}) \delta_{c,c'}), \quad (18)$$

where $\mathbf{v}_{nm}(\mathbf{k}) \equiv \langle n, \mathbf{k} | \mathbf{v} | m, \mathbf{k} \rangle$ is the velocity matrix element between Bloch states.

IV. TRANSITION AMPLITUDES

In the independent particle approximation, the transition amplitudes are

$$\Omega_{cv\kappa}^{(1-\text{free})} = i \frac{e}{2\hbar\omega} \mathbf{E}_{2\omega} \cdot \mathbf{v}_{cv}(\kappa), \quad (19)$$

and $\Omega_{cv\kappa}^{(2-\text{free})} = \sum_{c',v'} \Omega_{cc'vv'\kappa}^{(2-\text{free})}$, where

$$\Omega_{cc'vv'\kappa}^{(2-\text{free})} \equiv \left(\frac{e}{\hbar\omega} \right)^2 \frac{(\mathbf{E}_\omega \cdot (\mathbf{v}_{cc'}(\kappa) \delta_{v,v'} - \delta_{c,c'} \mathbf{v}_{v'v}(\kappa))) (\mathbf{E}_\omega \cdot \mathbf{v}_{c'v'}(\kappa))}{E_{c'v'}/\hbar - \omega(\kappa)}. \quad (20)$$

With excitonic effects included, using the perturbation $H_{\text{int}}(t)$ to second order gives the transition amplitudes

$$\Omega_{cv\kappa}^{(1)} = \frac{ie}{2\hbar\omega} \mathbf{E}_{2\omega} \cdot \langle cv\kappa | \mathbf{v} | 0 \rangle, \quad (21)$$

and

$$\Omega_{cv\kappa}^{(2)} = \left(\frac{e}{\hbar\omega} \right)^2 \sum_{c'v'\kappa'} \frac{(\mathbf{E}_\omega \cdot \langle cv\kappa | \mathbf{v} | c'v'\kappa' \rangle) (\mathbf{E}_\omega \cdot \langle c'v'\kappa' | \mathbf{v} | 0 \rangle)}{E_{c'v'}(\kappa')/\hbar - \omega}, \quad (22)$$

where the sum over intermediate states is over both bound and free excitons. The two-photon transition amplitude is more difficult to deal with due to the sum over intermediate states; however, in our set of approximations it has been done exactly.^{38,39,40}

In order to proceed analytically, it is common to use (17) and (18), and then make an expansion in \mathbf{k} of the velocity matrix elements $\mathbf{v}_{nm}(\mathbf{k})$ about the Γ point.^{30,36,37,38,39,40} However, due to the degeneracy at the Γ point, the coefficients of such an expansion can depend on the direction of \mathbf{k} .⁸¹ To proceed, we note that Wannier excitons have large spatial extent and hence only a small region of wavevectors is important for them, i.e., $A_{cv}^\kappa(\mathbf{k})$ is peaked in the region of \mathbf{k} near κ .⁶⁸ This is especially true for final states with energies above the band gap. Thus, we expand $\mathbf{v}_{nm}(\mathbf{k})$ about the Γ point, approached in the direction $\hat{\kappa}$,

$$v_{nm}^i(\mathbf{k}) = v_{nm}^i(\hat{\kappa}) + \mathbf{k} \cdot \nabla_{\mathbf{k}} v_{nm}^i(\hat{\kappa}) + \dots, \quad (23)$$

where $v_{nm}^i(\hat{\kappa}) \equiv \lim_{\lambda \rightarrow 0} \langle n, \Gamma | \mathbf{v} | m, \lambda\kappa \rangle$ and $\nabla_{\mathbf{k}} v_{nm}^i(\hat{\kappa}) \equiv \lim_{\lambda \rightarrow 0} \nabla_{\kappa} \langle n, \Gamma | \mathbf{v} | m, \lambda\kappa \rangle$.

Optical transitions due to the first term in (23) are called ‘allowed’, while those due to the second term are called ‘forbidden’. We restrict ourselves to materials for which the ‘allowed’ valence to conduction band transition does not vanish. Keeping only the ‘allowed’ term in (17),³⁶

$$\langle cv\kappa | \mathbf{v} | 0 \rangle = \mathbf{v}_{cv}(\hat{\kappa}) (\psi_{cv}^\kappa(\mathbf{r} = \mathbf{0}))^*. \quad (24)$$

For the intravalence and intraconduction band transitions, the first two terms of (23) in (18) give³⁹

$$\begin{aligned} \langle cv\mathbf{\kappa} | \mathbf{v} | c'v'\mathbf{\kappa}' \rangle &= [\delta_{v,v'} \mathbf{v}_{cc'}(\hat{\mathbf{\kappa}}) - \delta_{c,c'} \mathbf{v}_{v'v}(\hat{\mathbf{\kappa}})] \int \frac{d^3r}{L^3} (\psi_{cv}^{\mathbf{\kappa}}(\mathbf{r}))^* \psi_{c'v'}^{\mathbf{\kappa}'}(\mathbf{r}) \\ &\quad - [\delta_{v,v'} \nabla_{\mathbf{k}} v_{cc'}^i(\hat{\mathbf{\kappa}}) - \delta_{c,c'} \nabla_{\mathbf{k}} v_{v'v}^i(\hat{\mathbf{\kappa}})] i \int \frac{d^3r}{L^3} (\psi_{cv}^{\mathbf{\kappa}}(\mathbf{r}))^* \nabla \psi_{c'v'}^{\mathbf{\kappa}'}(\mathbf{r}). \end{aligned} \quad (25)$$

In particular,^{39,82}

$$\langle cv\mathbf{\kappa} | \mathbf{v} | cv\mathbf{\kappa} \rangle = \sum_{\mathbf{k}} (A_{cv}^{\mathbf{\kappa}}(\mathbf{k}))^* A_{cv}^{\mathbf{\kappa}}(\mathbf{k}) \frac{\hbar}{\mu_{cv}} \mathbf{k} = -i \frac{\hbar}{\mu_{cv}} \int \frac{d^3r}{L^3} (\psi_{cv}^{\mathbf{\kappa}}(\mathbf{r}))^* \nabla_{\mathbf{r}} \psi_{cv}^{\mathbf{\kappa}}(\mathbf{r}) = \hbar \mathbf{\kappa} / \mu_{cv}. \quad (26)$$

For Ge and for simple models of zincblende semiconductors that neglect lack of inversion symmetry, the first term in (25) always vanishes. This means that there are only ‘allowed-forbidden’ two-photon transitions (the interband transition is allowed, while the intraband transition is forbidden). When the first term is nonvanishing, there are ‘allowed-allowed’ two-photon transitions. In principle, for materials that lack a center of inversion, there is also a small contribution to the ‘allowed-forbidden’ two-photon transition from the first term in (25) and the term in $\langle cv\mathbf{\kappa} | \mathbf{v} | 0 \rangle$ that comes from the second term in (23); we neglect it in what follows, but note that when compared to the dominant ‘allowed-forbidden’ contribution that we consider here, it has a different Coulomb enhancement but the same intrinsic phase (see Eq. 2.32 of Rustagi *et al.*).³⁹

We write $\Omega_{cv\mathbf{\kappa}}^{(2)} = \Omega_{cv\mathbf{\kappa}}^{(2:\text{a-f})} + \Omega_{cv\mathbf{\kappa}}^{(2:\text{a-a})}$, and discuss the ‘allowed-forbidden’ and ‘allowed-allowed’ transitions separately.

Using (16), (24), and (21), the one-photon transition amplitude is³⁶

$$\Omega_{cv\mathbf{\kappa}}^{(1)} = \Omega_{cv\mathbf{\kappa}}^{(1-\text{free})} \exp\left(\frac{\pi}{2a_{cv\mathbf{\kappa}}}\right) \Gamma\left(1 - \frac{i}{a_{cv\mathbf{\kappa}}}\right), \quad (27)$$

where only the ‘allowed’ term is kept in $\Omega_{cv\mathbf{\kappa}}^{(1-\text{free})}$. The transition is to an *s*-wave. The one-photon absorption coefficient is proportional to the norm of $\Omega_{cv\mathbf{\kappa}}^{(1)}$ [see (8) and (9)].³⁶

For ‘allowed-forbidden’ two-photon transitions, substituting (24) and the second term of (25) into (22),

$$\Omega_{cv\mathbf{\kappa}}^{(2:\text{a-f})} = \frac{e^2}{\omega^2 \hbar} \sum_{c'v'} (\mathbf{E}_{\omega} \cdot \mathbf{v}_{c'v'}(\hat{\mathbf{\kappa}})) E_{\omega}^i (\delta_{v,v'} \nabla_{\mathbf{k}} v_{cc'}^i(\hat{\mathbf{\kappa}}) - \delta_{c,c'} \nabla_{\mathbf{k}} v_{v'v}^i(\hat{\mathbf{\kappa}})) \cdot \mathbf{M}_{cc'vv'}(\mathbf{\kappa}), \quad (28)$$

where

$$\mathbf{M}_{cc'vv'}(\mathbf{\kappa}) \equiv -i \int d^3r (\psi_{cv}^{\mathbf{\kappa}}(\mathbf{r}))^* \nabla G_{c'v'}(\mathbf{r}, \mathbf{0}; \hbar\omega - E_{c'v'}^g), \quad (29)$$

and we have used the Coulomb Green function,

$$G_{cv}(\mathbf{r}, \mathbf{r}'; \Omega) = \frac{1}{L^3} \sum_{\kappa} \frac{\psi_{cv}^{\kappa}(\mathbf{r}) (\psi_{cv}^{\kappa}(\mathbf{r}'))^*}{E_{cv}(\kappa) - E_{cv}^g - \Omega},$$

which is known analytically.³⁸ In particular,

$$G_{cv}(\mathbf{r}, \mathbf{0}; \hbar\omega - E_{cv}^g) = \frac{\mu_{cv}}{2\pi r \hbar^2} \Gamma(1 - \gamma_{cv}) W_{\gamma_{cv}, \frac{1}{2}}\left(\frac{2r}{a_{cv}\gamma_{cv}}\right), \quad (30)$$

where we define

$$\gamma_{cv} \equiv \sqrt{\frac{B_{cv}}{E_{cv}^g - \hbar\omega}},$$

$B_{cv} = \hbar^2/(2\mu_{cv}a_{cv}^2)$ is the exciton binding energy, and $W_{\gamma, 1/2}(z)$ is a Whittaker function with the integral representation

$$W_{\gamma, 1/2}(z) = \frac{ze^{-\frac{z}{2}}}{\Gamma(1 - \gamma)} \int_0^\infty dt \left(\frac{1+t}{t}\right)^\gamma e^{-zt}. \quad (31)$$

Since the Green function depends only on the magnitude of \mathbf{r} , only the p -wave of the final state survives the integral in Eq. (29) over the angles of \mathbf{r} , $\int d\Omega P_1(\hat{\mathbf{r}} \cdot \hat{\boldsymbol{\kappa}}) \hat{\mathbf{r}} = 4\pi \hat{\boldsymbol{\kappa}}/3$. The integral over r can be done using³⁸

$$\int_0^\infty r^{\sigma-1} e^{-pr} {}_1F_1(\alpha; \sigma; \lambda r) dr = \Gamma(\sigma) \frac{p^{\alpha-\sigma}}{(p - \lambda)^\alpha}. \quad (32)$$

The final result is

$$\Omega_{cv\kappa}^{(2:a-f)} = \exp\left(\frac{\pi}{2a_{cv}\kappa}\right) \Gamma\left(2 - \frac{i}{a_{cv}\kappa}\right) \sum_{c'v'} N_{cc'vv'}^{(a-f)}(\kappa) \Omega_{cc'vv'\kappa}^{(2-free)}, \quad (33)$$

where only the ‘allowed-forbidden’ term is kept in $\Omega_{cc'vv'\kappa}^{(2-free)}$, and

$$N_{cc'vv'}^{(a-f)}(\kappa) \equiv (1 + a_{c'v'}^2 \kappa^2 \gamma_{c'v'}^2) 2 \int_0^1 \frac{S \left(\frac{1+S}{1-S}\right)^{\gamma_{c'v'}} \exp\left(-\frac{2}{a_{cv}\kappa} \arctan(a_{c'v'} \kappa \gamma_{c'v'} S)\right)}{(1 + a_{c'v'}^2 \kappa^2 \gamma_{c'v'}^2 S^2)^2} dS. \quad (34)$$

For ‘allowed-allowed’ two-photon transitions, substituting (24) and the first term of (25) into (22),

$$\begin{aligned} \Omega_{cv\kappa}^{(2:a-a)} &= \left(\frac{e}{\hbar\omega}\right)^2 \sum_{c'v'} \mathbf{E}_\omega \cdot [\delta_{vv'} v_{cc'}^i(\hat{\boldsymbol{\kappa}}) - \delta_{c,c'} v_{v'v}^i(\hat{\boldsymbol{\kappa}})] \mathbf{E}_\omega \cdot \mathbf{v}_{c'v'}(\hat{\boldsymbol{\kappa}}) \\ &\times \hbar \int d^3r (\psi_{cv}^{\kappa}(\mathbf{r}))^* G_{c'v'}(\mathbf{r}, \mathbf{0}; \hbar\omega - E_{c'v'}^g). \end{aligned}$$

Since $G_{c'v'}$ depends only on the magnitude of \mathbf{r} [Eq. (30)], only the s part of the final state will survive the integration over angles of \mathbf{r} . Again we use (31) for the Whittaker function.

The integral over the magnitude of \mathbf{r} can be done using an identity obtained by taking a derivative with respect to p of both sides of (32). Finally,

$$\Omega_{cv\kappa}^{(2:a-a)} = \exp\left(\frac{\pi}{2a_{cv}\kappa}\right) \Gamma\left(1 - \frac{i}{a_{cv}\kappa}\right) \sum_{c'v'} \Omega_{cc'vv'\kappa}^{(2-free)} N_{cc'vv'}^{(a-a)}(\kappa), \quad (35)$$

where only the ‘allowed-allowed’ term is kept in $\Omega_{cc'vv'\kappa}^{(2-free)}$, and

$$\begin{aligned} N_{cc'vv'}^{(a-a)}(\kappa) &\equiv (1 + (a_{c'v'}\kappa\gamma_{c'v'})^2) 2 \\ &\times \int_0^1 S \left(1 - S \frac{a_{c'v'}\gamma_{c'v'}}{a_{cv}}\right) \left(\frac{1+S}{1-S}\right)^{\gamma_{c'v'}} \frac{\exp\left(-\frac{2}{a_{cv}\kappa} \arctan(a_{c'v'}\kappa\gamma_{c'v'}S)\right)}{(1 + (a_{c'v'}\kappa\gamma_{c'v'}S)^2)^2} dS. \end{aligned} \quad (36)$$

This agrees with Eq. 2.28 of Rustagi,³⁹ but note that we have defined $N_{cc'vv'}^{(a-a)}(\kappa) = (1 + (a_{c'v'}\kappa\gamma_{c'v'})^2) I_{s,k}(\kappa)$, where $I_{s,k}(\kappa)$ is given, with a typographical error, in Eq. 2.25 of that paper.

The factors $N_{cc'vv'}^{(a-f)}$ and $N_{cc'vv'}^{(a-a)}$, which appear in (34) and (36) are the enhancements due to the Coulomb interaction in the intermediate states; they are discussed further in Appendix A.

V. RESULTS

The one- and two-photon transition amplitudes were presented in the previous section on the basis of an expansion in \mathbf{k} of the Bloch state velocity matrix elements. The ‘allowed’ one-photon transition amplitude $\Omega^{(1)}$ is in (27), the ‘allowed-forbidden’ two-photon transition amplitude is in (33), and the ‘allowed-allowed’ two-photon transition amplitude is in (35). From them, $\mathbf{D}_{cv\kappa}^{(1)}$ and $\mathbf{D}_{cv\kappa}^{(2)}$ may be extracted by comparison with the definitions in (5) and (6).

A. Current injection

The ‘1+2’ current injection is dominated by interference of ‘allowed’ one-photon transitions and ‘allowed-forbidden’ two-photon transitions.⁸⁰ Substituting these into (7), and using the Gamma function identities $\Gamma(x+1) = x\Gamma(x)$ and

$$\Gamma(1-ix)\Gamma(1+ix) = \pi x / \sinh(\pi x), \quad (37)$$

yields our final result for the current injection tensor

$$\eta_{(I)}^{ijkl} = \sum_{c,v} \left(1 + \frac{i}{a_{cv}\kappa_{cv}} \right) \Xi(a_{cv}\kappa_{cv}) \sum_{c',v'} N_{cc'vv'}^{(\text{a-f})}(\kappa_{cv}) \eta_{cc'vv'}^{ijkl}, \quad (38)$$

where

$$\kappa_{cv} \equiv \frac{1}{a_{cv}} \sqrt{\frac{2\hbar\omega - E_{cv}^g}{B_{cv}}}, \quad (39)$$

$$\Xi(x) \equiv \frac{(\pi/x) \exp(\pi/x)}{\sinh(\pi/x)} = \frac{2\pi}{x} (1 - \exp(-2\pi/x))^{-1}, \quad (40)$$

and

$$\eta_{cc'vv'}^{ijkl} \equiv \frac{2\pi e}{L^3} \sum_{\boldsymbol{\kappa}} \Delta_{cv}^i(\boldsymbol{\kappa}) \left(D_{cc'vv'\boldsymbol{\kappa}}^{(2\text{-free})*} \right)^{jk} \left(D_{cv\boldsymbol{\kappa}}^{(1\text{-free})} \right)^l \delta(2\omega - E_{cv}(\boldsymbol{\kappa})/\hbar), \quad (41)$$

with $\Delta_{cv}(\boldsymbol{\kappa}) \equiv (\mathbf{v}_{cc}(\boldsymbol{\kappa}) - \mathbf{v}_{vv}(\boldsymbol{\kappa})) = \hbar\boldsymbol{\kappa}/\mu_{cv}$ and

$$\left(D_{cc'vv'\boldsymbol{\kappa}}^{(2\text{-free})} \right)^{jk} = \left(\frac{e}{\hbar\omega} \right)^2 \frac{\{(\mathbf{v}_{cc'}(\boldsymbol{\kappa})\delta_{v,v'} - \delta_{c,c'}\mathbf{v}_{v'v}(\boldsymbol{\kappa})), \mathbf{v}_{c'v'}(\boldsymbol{\kappa})\}^{jk}}{E_{c'v'}(\boldsymbol{\kappa})/\hbar - \omega}, \quad (42)$$

where $\{\mathbf{v}_1, \mathbf{v}_2\}^{ij} \equiv (v_1^i v_2^j + v_1^j v_2^i)/2$ and

$$\left(D_{cv\boldsymbol{\kappa}}^{(1\text{-free})} \right)^l = i \frac{e}{2\hbar\omega} v_{cv}^l(\boldsymbol{\kappa}). \quad (43)$$

Note that only the ‘allowed’ part of (43) and the ‘allowed-forbidden’ part of (42) should be retained for a consistent solution. We have written (38) to separate the parts due to the electron-hole interaction. In the independent particle approximation, the current injection tensor $\eta_{(I\text{-free})}^{ijkl}$ is¹¹

$$\eta_{(I\text{-free})}^{ijkl} = \sum_{c,c',v,v'} \eta_{cc'vv'}^{ijkl}; \quad (44)$$

it is evaluated for parabolic bands in Appendix B.

For GaAs, we present in Fig. 1 the magnitude of $\eta_{(I)}^{xxxx}$, based on $\eta_{cc'vv'}^{xxxx}$ calculated by two methods. The first method, described in Appendix B, uses isotropic parabolic bands and includes only two-band terms; it uses effective mass ratios for conduction, heavy hole, light hole, and split-off bands of 0.067, 0.51, 0.082, and 0.154 respectively, $E_P = 27.86$ eV, the fundamental band gap E_g is 1.519 eV, and valence band spin-orbit splitting is 0.341 eV.^{83,84} The second method solves the $8 \times 8 \mathbf{k} \cdot \mathbf{p}$ Hamiltonian including remote band effects, but in a spherical approximation with warping and spin-splitting neglected by replacing γ_2 and γ_3 with $\tilde{\gamma} \equiv (2\gamma_2 + 3\gamma_3)/5$ ⁷⁸; the calculation is nonperturbative in \mathbf{k} (hence it includes band nonparabolicity) and it includes both two- and three-band terms in the two-photon

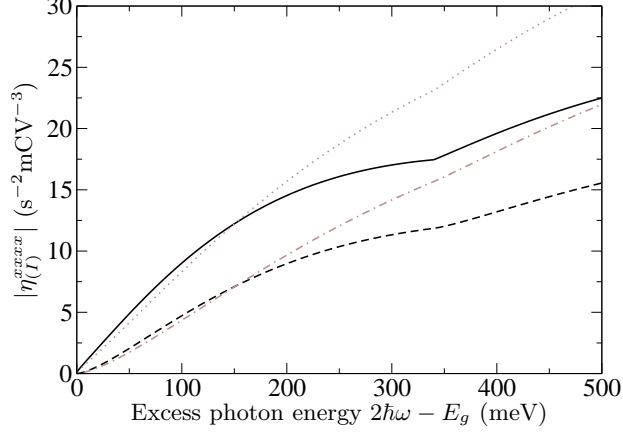


FIG. 1: Magnitude of the diagonal element of the current injection tensor for GaAs with [Eq. (38)] and without [Eq. (44)] excitonic effects. The grey dotted and dash-dotted lines are based on a parabolic band calculation of $\eta_{cc'vv'}^{xxxx}$ that only includes two-band terms; the dotted line includes excitonic effects, while the dash-dotted line does not. The black solid and dashed lines are based on $\eta_{cc'vv'}^{xxxx}$ calculated with a nonperturbative solution of the $8 \times 8 \mathbf{k} \cdot \mathbf{p}$ Hamiltonian; the solid line includes excitonic effects, while the dashed line does not.

amplitude.⁸⁰ The solid and dotted lines in Fig. 1 are calculated with (38), and hence include excitonic effects; the Coulomb enhancement part of the calculation uses $B_{cv} = 4.2 \text{ meV}$ ⁸⁵ and the band parameters listed above. Note that the solid black line in Fig. 1 is inconsistent in the sense that the Coulomb enhancement is based on an expansion in \mathbf{k} , whereas the free-particle result that it enhances is nonperturbative in \mathbf{k} ; nevertheless, such an approach has given good agreement with experiments for one- and two-photon absorption.^{86,87}

The Coulomb enhancement of $\eta_{(I)}$ can clearly be seen in Fig. 1. There is a kink in each curve at excess photon energy 341 meV corresponding to the onset of transitions from the *so* band. At higher energies, the Coulomb enhancement of *so* transitions is larger than the Coulomb enhancements of *hh* and *lh* transitions, since the former transitions are to conduction band states with lower energy. Hence, the kink in $\eta_{(I)}$ is enhanced by excitonic effects.

We extract the intrinsic phase of $\eta_{(I)}^{xxxx}$ using (2). The solid line in Fig. 2 is the intrinsic phase of $\eta_{(I)}^{xxxx}$ calculated for GaAs with the nonperturbative $8 \times 8 \mathbf{k} \cdot \mathbf{p}$ Hamiltonian band model; the result for the parabolic band model is nearly identical. Since we have used a spherical exciton model, the intrinsic phase is the same for all components of $\eta_{(I)}^{ijkl}$. The

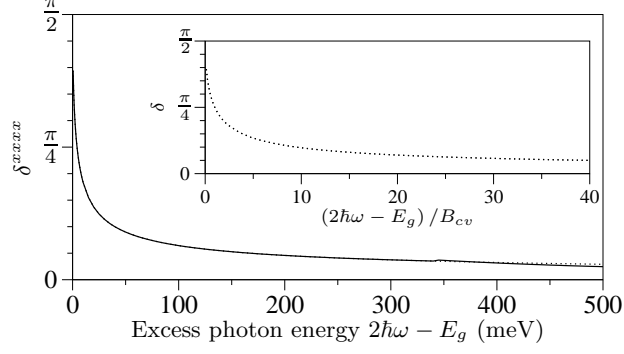


FIG. 2: Phase shift of the current (intrinsic phase of $\eta_{(I)}^{xxx}$) in GaAs due to excitonic effects. The solid line is calculated with Eqs. (2) and (38), and the dotted line is calculated with Eq. (45). The inset is Eq. (45) plotted in scaled units.

intrinsic phase has its maximum value of $\pi/2$ at the band edge, and goes to zero as the light frequency increases. The decrease is smooth except for a small kink at the onset of transitions from the *so* band. In fact, for excess photon energies less than the split-off energy, the intrinsic phase has the simple analytic form

$$\delta(\omega) = \arctan \left(\sqrt{\frac{B_{cv}}{2\hbar\omega - E_g}} \right). \quad (45)$$

Equation (45) is plotted as the dotted line in Fig. 2; compared to the solid line, it is identical below the onset of *so* transitions, and it makes a good approximation above the the onset of *so* transitions. Since (45) only depends on the excess photon energy scaled by the exciton binding energy, we plot it as a function of this scaled energy in the inset of Fig. 2; it is useful for finding the intrinsic phase of materials other than GaAs.

In $\eta_{(I)}$ [Eq. (38)], the two- and three-band terms have different intermediate state Coulomb enhancement $N_{cc'vv'}^{(a-f)}$. For many materials, however, $N_{cc'vv'}^{(a-f)}$ is approximately equal for all the terms $\eta_{cc'vv'}^{ijkl}$ that contribute significantly to the total $\eta_{(I-free)}^{ijkl}$, as shown in Appendix A for GaAs. Thus, at photon energies for which transitions from the heavy- and light-hole bands dominate η , the Coulomb enhancement becomes approximately independent of the sum over bands and we can make the simplification

$$\eta_{(I)}^{ijkl} \approx F_{a-f}^{(I)} \exp(i\delta) \eta_{(I-free)}^{ijkl}, \quad (46)$$

where the intrinsic phase is given by (45), and

$$F_{a-f}^{(I)}(\omega) \equiv \Xi(a_{cv}\kappa_{cv}) \sqrt{1 + (a_{cv}\kappa_{cv})^{-2} N_{ccvv}^{(a-f)}(\kappa_{cv})}, \quad (47)$$

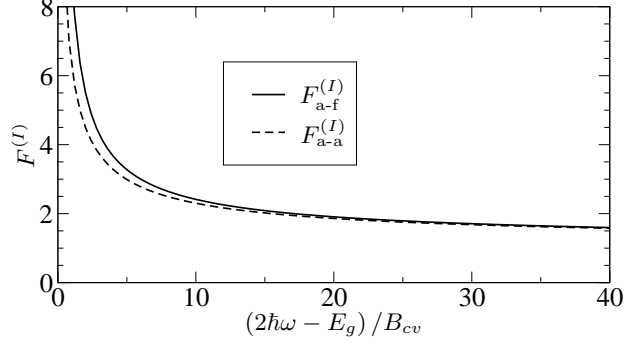


FIG. 3: Approximate Coulomb enhancement factors. The solid line, applicable to current and spin current control, is $F_{a-f}^{(I)}$ [Eq. (47)] with $N_{ccvv}^{(a-f)} = 1$, and the dotted line, applicable to carrier population and spin control is $F_{a-a}^{(I)}$ [Eq. (52)] with $N_{ccvv}^{(a-a)} = 1$

The Coulomb enhancement factor $F_{a-f}^{(I)}(\omega)$ is plotted in Fig. 3 with the approximation that $N_{ccvv}^{(a-f)} = 1$ (see Appendix A).

B. Carrier population control

The ‘1+2’ carrier population control is dominated by interference of ‘allowed’ one-photon transitions and ‘allowed-allowed’ two-photon transitions.^{20,22,80} Substituting these into (12), and using the Gamma function identity (37), we find

$$\xi_{(I)}^{ijk} = \sum_{c,v} \Xi(a_{cv}\kappa_{cv}) \sum_{c'v'} N_{cc'vv'}^{(a-a)}(\kappa_{cv}) \xi_{cc'vv'}^{ijk}, \quad (48)$$

where

$$\xi_{cc'vv'}^{ijk} = \frac{2\pi e}{L^3} \sum_{\kappa} \left(D_{cc'vv'\kappa}^{(2\text{-free})*} \right)^{jk} \left(D_{cv\kappa}^{(1\text{-free})} \right)^l \delta(2\omega - E_{cv}(\kappa)/\hbar) \quad (49)$$

and $D_{cc'vv'\kappa}^{(2\text{-free})}$ and $D_{cv\kappa}^{(1\text{-free})}$ are given by (42) and (43). Note that only the ‘allowed’ part of (43) and the ‘allowed-allowed’ part of (42) should be retained for a consistent solution. In the independent particle approximation,

$$\xi_{(I\text{-free})}^{ijk} = \sum_{c'v'} \xi_{cc'vv'}^{ijk}. \quad (50)$$

Thus, population control has a Coulomb enhancement due to excitonic effects, but no phase shift.

Note that (48) gives the population control tensor at final energies above the band edge. There can also be population control of bound excitons when both one- and two-photon

transitions are to the same excitonic state. This can occur, for example, at s excitons due to allowed-allowed two-photon transitions⁴¹ interfering with allowed one-photon transitions.

If $N_{cc'vv'}^{(a-a)}(\kappa_{cv})$ is approximately the same for all the terms that significantly contribute to $\xi_{(I)}$, then, at photon energies for which transitions from the heavy and light hole bands dominate $\xi_{(I)}$, the Coulomb enhancement becomes approximately independent of the sum over bands, and we can make the simplification,

$$\xi_{(I)}^{ijk} \approx F_{a-a}^{(I)} \xi_{(I\text{-free})}^{ijk}, \quad (51)$$

where

$$F_{a-a}^{(I)}(\omega) \equiv \Xi(a_{cv}\kappa_{cv}) N_{ccvv}^{(a-a)}(\kappa_{cv}). \quad (52)$$

The Coulomb enhancement factor $F_{a-a}^{(I)}(\omega)$ is plotted in Fig. 3 with the approximation that $N_{ccvv}^{(a-a)} = 1$ (see Appendix A).

C. Spin current injection and spin control

The ‘1+2’ spin current is dominated by interference of ‘allowed’ one-photon transitions and ‘allowed-forbidden’ two-photon transitions, whereas ‘1+2’ spin control is dominated by interference of ‘allowed’ one-photon transitions and ‘allowed-allowed’ two-photon transitions.⁸⁰ Under the approximations that led to (46) and (51), the spin current injection pseudotensor is

$$\mu_{(I)}^{ijklm} = F_{a-f}^{(I)} \exp(i\delta) \mu_{(I\text{-free})}^{ijklm}, \quad (53)$$

where $F_{a-f}^{(I)}$ is given by (47), δ is given by (45), and $\mu_{(I\text{-free})}$ is the spin current injection pseudotensor in the independent particle approximation. Under similar approximations, the spin control pseudotensor is

$$\zeta_{(I)}^{ijkl} = F_{a-a}^{(I)} \zeta_{(I\text{-free})}^{ijkl}, \quad (54)$$

where $F_{a-a}^{(I)}$ is given by (52), and $\zeta_{(I\text{-free})}$ is the spin control pseudotensor in the independent particle approximation. Spin control, like carrier population control, has a Coulomb enhancement but no phase shift. There can also be spin control of bound excitons, but it has not been included in (54).

VI. DISCUSSION

We now examine the relationship between the Coulomb enhancements of the ‘1+2’ processes and of one- and two-photon absorption; the latter are denoted by $F^{(1)}$ and $F^{(2)}$ so that for $i \in \{1, 2\}$, $\dot{n}^{(i)} = \dot{n}_{\text{free}}^{(i)} F^{(i)}$. The relationship is particularly simple at photon energies for which transitions from the heavy- and light-hole bands are dominant and intermediate state Coulomb enhancement is the same for each significant term in the sum over intermediate states. The Coulomb enhancements for the ‘1+2’ processes are then given by (47) and (52). For one-photon absorption, $F^{(1)} = \Xi(a_{cv}\kappa_{cv})$.³⁶ In noncentrosymmetric semiconductors, two-photon absorption is dominated by allowed-allowed transitions just above the band gap, and by allowed-forbidden transitions at higher final energies; the cross-over point in GaAs is a few meV above the band gap.⁸⁸ At photon energies for which allowed-allowed transitions dominate two-photon absorption, from (35),

$$F^{(2)} = \Xi(a_{cv}\kappa_{cv}) (N_{ccvv}^{(a-a)}(\kappa_{cv}))^2, \quad (55)$$

and thus

$$F_{a-a}^{(I)} = \sqrt{F^{(1)}F^{(2)}} \text{ and } F_{a-f}^{(I)} = C\sqrt{F^{(1)}F^{(2)}}, \quad (56)$$

where $C \equiv (N_{ccvv}^{(a-f)}(\kappa_{cv})/N_{ccvv}^{(a-a)}(\kappa_{cv}))\sqrt{1 + (a_{cv}\kappa_{cv})^{-2}}$, while at photon energies for which allowed-forbidden transitions dominate two-photon absorption, from (33),

$$F^{(2)} = \Xi(a_{cv}\kappa_{cv}) (1 + (a_{cv}\kappa_{cv})^{-2}) (N_{ccvv}^{(a-f)}(\kappa_{cv}))^2, \quad (57)$$

and thus

$$F_{a-a}^{(I)} = (1/C)\sqrt{F^{(1)}F^{(2)}} \text{ and } F_{a-f}^{(I)} = \sqrt{F^{(1)}F^{(2)}}. \quad (58)$$

Note that, based on Appendix A, $C \approx \sqrt{1 + B_{cv}/(2\hbar\omega - E_g)}$, which is the ratio of the two curves in Fig. 3. In centrosymmetric semiconductors, there are no allowed-allowed transitions, and only (58) applies.

The ‘1+2’ processes are often described by ratios. For example, a useful quantity to describe the current is the swarm velocity,^{56,89} defined as the average velocity per injected electron-hole pair

$$\mathbf{v}_{\text{swarm}} \equiv \frac{(d\mathbf{J}/dt)}{e(dn/dt)}.$$

The swarm velocity is a maximum when the relative intensities of the two colors are chosen such that $\dot{n}_{2\omega} = \dot{n}_{\omega}$; returning to (4), if one associates the one- and two-photon amplitudes

with the arms of an effective interferometer, this condition corresponds to balancing that interferometer. For fields co-linearly polarized along $\hat{\mathbf{x}}$, the maximum swarm speed is

$$v_{\text{swarm}} = \frac{1}{e} \frac{|\eta_{(I)}^{xxxx}|}{\sqrt{\xi_{(1)}^{xx} \xi_{(2)}^{xxxx}}}. \quad (59)$$

A useful quantity to describe pure spin currents is the maximum spin separation distance¹⁶; it is proportional to $\mu_{(I)}/\sqrt{\xi_{(1)}\xi_{(2)}}$. As a consequence of (58), the maximum swarm speed, and the maximum spin separation distance, are *unaffected* by excitonic effects when allowed-forbidden transitions dominate two-photon absorption.⁹⁰ However, close to the band edge, where allowed-allowed transitions dominate two-photon absorption, excitonic effects increase these ratios by a factor C over their value in the independent particle approximation. In contrast, as a consequence of (58), excitonic effects do not affect the maximum control ratio for population and spin control ($\xi_{(I)}/\sqrt{\xi_{(1)}\xi_{(2)}}$ and $\zeta_{(I)}/\sqrt{\xi_{(1)}\xi_{(2)}}$ respectively)^{19,21,22} close to the band edge and decrease them by a factor C at higher photon energies for which allowed-forbidden transitions dominate two-photon absorption.

In the terminology of Seideman,²⁶ the excitonic phase shift of the ‘1+2’ current and spin current is a direct phase shift. It is due to the complex nature of the final state as it appears in the transition amplitudes. Thus it can be understood in terms of the partial wave phase shifts of the final state caused by the Coulomb potential between electron and hole. The Coulomb interaction is rather unique due to its long range nature, so we first suppose the potential between the electron and hole falls off more rapidly than $1/C$. In that simpler problem, the final state wave function is written as

$$\psi_{\boldsymbol{\kappa}}(\mathbf{r}) = \sum_{l=0}^{\infty} i^l e^{-i\delta_l(\kappa)} (2l+1) \frac{u_{\kappa,l}(r)}{r} P_l\left(\frac{\mathbf{r} \cdot \boldsymbol{\kappa}}{r\kappa}\right),$$

where the $u_{\kappa,l}(r)$ are real.⁷² If the potential between the particles is ignored, then the partial wave phase shifts, $\delta_l(\kappa)$ are zero. The allowed one-photon pathway reaches an s wave, while the allowed-forbidden two-photon pathway reaches a p wave. Substituting this form for the wave function into the one- and two-photon transition amplitudes, yields $\Omega_{\boldsymbol{\kappa}}^{(1)} = \Omega_{\boldsymbol{\kappa}}^{(1\text{-free})} e^{i\delta_0(\kappa)} f_0(\kappa)$ for the one-photon rate, where $f_0(\kappa)$ is real and depends on $u_{\kappa,0}(r)$, and $\Omega_{\boldsymbol{\kappa}}^{(2\text{:a-f})} = \Omega_{\boldsymbol{\kappa}}^{(2\text{-free})} e^{i\delta_1(\kappa)} f_1(\kappa)$ for the two-photon rate, where $f_1(\kappa)$ is real and depends on $u_{\kappa,0}(r)$ and $u_{\kappa,1}(r)$. Here $\Omega_{\boldsymbol{\kappa}}^{(i\text{-free})}$ is the i -photon transition amplitude when the potential between the particles is ignored. It is then straightforward to see from (7) that the

relative shift of the partial waves is responsible for the phase shift of the current and spin current. That is,

$$\delta = \delta_0 - \delta_1. \quad (60)$$

The use of ionization states as opposed to scattering states was important to get the correct sign of the intrinsic phase. With scattering states, one would find $\delta = \delta_1 - \delta_0$.

Due to the long-range nature of the Coulomb potential, the partial wave phase shifts have a logarithmic r dependent part, but it is the same for all partial waves and thus does not appear in the relative phase. The part of the Coulomb partial wave phase shift $\delta_l(\kappa)$ that does not depend on r is $\arg(\Gamma(l+1+i/(a_{cv}\kappa)))$ ^{72,82}; when inserted into (60), this reproduces (45). In contrast, the allowed-allowed two-photon pathway reaches an s wave and thus there is no phase shift for population control or spin control.

The expression (60) for the intrinsic phase in terms of the scattering phases is particularly simple, since each pathway connects to only a single parity. This contrasts with ‘1+2’ ionization from an atomic s state, for which the one-photon transition is to a p wave and the two-photon transition is to both s and d waves; the intrinsic phase is thus a weighting of the p - s and p - d partial wave shifts.²⁸ Materials for which the first term in (23) is forbidden (Cu_2O is an example) have these same selection rules^{36,38,39}; hence, they will have an intrinsic phase with a similar weighting.

The absence of a phase shift in population control can be connected to a symmetry of the second order nonlinear optical susceptibility. From considerations of energy transfer and macroscopic electrodynamics, $\xi_{(I)}$ is related to the nonlinear susceptibility $\chi^{(2)}$ by

$$\xi_{(I)}^{ijk} = (i\epsilon_0/\hbar) [\chi^{(2)kij}(2\omega; -\omega, -\omega) - \chi^{(2)jki}(-\omega; 2\omega, -\omega)]. \quad (61)$$

In the independent particle approximation,⁶³

$$\chi^{(2)ijk}(2\omega; -\omega, -\omega) = [\chi^{(2)jik}(-\omega; 2\omega, -\omega)]^*, \quad (62)$$

which is a generalization of overall permutation symmetry to resonant absorption. As a result of (62), Fraser *et al.* showed that $\xi_{(I)}$ is proportional to $\text{Im}\chi^{(2)}$, and is thus purely real.¹⁹ Our result that $\xi_{(I)}$ remains real when excitonic effects are included suggests that (62) holds more generally. In fact, it can be shown that (62) holds for any Hamiltonian symmetric under time-reversal so long as $\hbar\omega$ is not resonant.

VII. SUMMARY AND OUTLOOK

We have extended the theory of interband ‘1+2’ processes in bulk semiconductors to include the electron-hole interaction. Following previous theories,^{11,13,17,19,21} we have used a framework based on (i) a separation of the initial carrier photoinjection and the subsequent carrier scattering, and (ii) a perturbative expansion in the optical field amplitudes, with injection rates obtained in a Fermi’s golden rule limit for the bichromatic field. The injection rates for carrier population control, spin control, current injection, and spin current injection, have been described phenomenologically by tensors $\xi_{(I)}$, $\zeta_{(I)}$, $\eta_{(I)}$, and $\mu_{(I)}$, respectively.^{11,17,19,21,22} Like previous theories, we have used the long-wavelength limit, and neglect nonlocal corrections to the interaction Hamiltonian. But whereas previous theories of ‘1+2’ photoinjection used the independent particle approximation, we have included excitonic effects. We have shown that excitonic effects cause (i) an enhancement of each ‘1+2’ process, and (ii) a phase shift for current injection and spin current injection. Our main results, the modifications of the aforementioned tensors relative to the independent particle approximation are given in (46), (51), (53), and (54). These particularly simple results are valid at photon energies for which transitions from the heavy- and light-hole bands are dominant; more general results are given for $\eta_{(I)}$ and $\xi_{(I)}$ in (38) and (48).

Our results are based on the effective mass model of Wannier excitons; degenerate bands are included, but we use a spherical approximation to the exciton Hamiltonian, and we neglect envelope-hole coupling. This is a good approximation for many typical semiconductors, including GaAs, since the electron-hole envelope function extends over many unit cells due to the screening of the Coulomb interaction by the static dielectric constant.^{42,70,77,78,79} As a consequence of making the spherical approximation, the phase shifts and Coulomb enhancements we find in this paper are independent of crystal orientation.

Also, our results are limited to low excess photon energy since (i) the Wannier exciton Hamiltonian assumes parabolic Bloch bands, and (ii) we have truncated the expansion in \mathbf{k} of the Bloch state velocity matrix elements, which is the basis of the transition amplitude expansion. By comparing the black dashed line and grey dash-dotted line in Fig. 1, one sees that higher order terms in \mathbf{k} (for both bands and velocities) are important in GaAs for excess photon energies greater than about 200 meV. This can then be considered the limit of validity of our calculation. However, combining the Coulomb enhancement calculated

assuming parabolic bands with the nonperturbative independent particle approximation result (as was done for the solid black line in Fig. 1) likely gives a good approximation for a few hundred more meV; this was the case for one- and two-photon absorption.^{86,87}

It is interesting to ask if there are other sources of intrinsic phases to the current (or spin current) besides the one that we have identified here, as these may produce spectral features in the intrinsic phase. One possibility is the coupling between bound *so-c* excitons and the unbound *hh-c* or *lh-c* excitons, since it is known that the intrinsic phase can show spectral features near a resonance.²⁷ Another possibility is the envelope-hole coupling between the continua of unbound *hh-c* and *lh-c* excitons that was neglected in our treatment. The effect of coupled continua in the general theory of ‘ $n + m$ ’ phase shifts has not been considered to date.

Finally, we note that the intrinsic phase and Coulomb enhancement may be greater in reduced dimensional systems, which have greater exciton binding energies. The carrier-carrier Coulomb interaction was included in the theory for ‘ $1 + 2$ ’ control of electrons in biased asymmetric quantum wells, although the intrinsic phase was not studied.¹⁰

APPENDIX A: INTERMEDIATE STATE COULOMB ENHANCEMENT

Consider the functions $N^{(a-f)}$ and $N^{(a-a)}$, which appear in (34) and (36); we refer to them collectively as N . First, note that due to the energy conserving delta function in (7), κ will be equal to κ_{cv} [see Eq. (39)], and thus N is a function only of ω , E_{cv}^g , $E_{c'v'}^g$, μ_{cv} , and $\mu_{c'v'}$. Second, note that N is defined so that if the electron-hole attraction is turned off, for example by letting $\epsilon \rightarrow \infty$, then $N \rightarrow 1$.⁹¹ This allows N to be identified as part of the Coulomb enhancement. In particular, N is the enhancement due to the Coulomb interaction in the intermediate states; if the Coulomb interaction is neglected for the intermediate states, $N = 1$.⁴¹ [Note that Lee and Fan⁴⁰ did not allow for $v' \neq v$ in N (related to J_j in their notation).]

Since the integrand is smooth for the parameter range of interest, numerical integration of N is straightforward; however, it need not be undertaken. Further simplification is possible since the parameter γ can be considered to be much less than one. Since most materials have an exciton binding energy that is much smaller than the band gap, $\hbar\omega$ is detuned from the band edge by many exciton binding energies at photon energies consistent with the

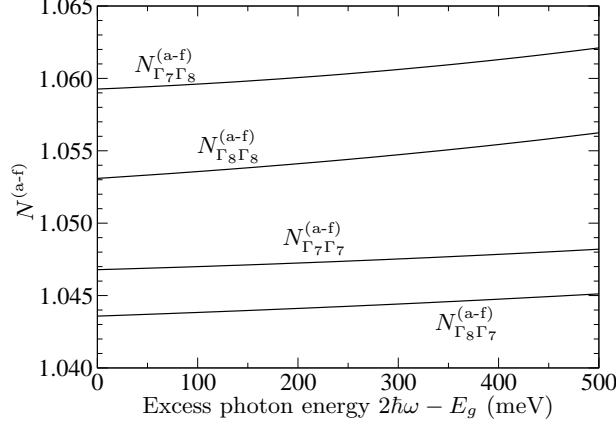


FIG. 4: The factor $N^{(a-f)}$ [intermediate state Coulomb enhancement, see (33)] for GaAs. The first (second) subscript is v (v'); subscripts for $c = c' = \Gamma_6$ are not shown; Γ_8 denotes the heavy and light hole bands, and Γ_7 denotes the split off band.

approximations made here. In GaAs, for example, when $2\hbar\omega$ is within 500 meV of the gap, γ is at most 0.09. An expansion of $N^{(a-f)}$ for small γ ,

$$N^{(a-f)} = 1 + \frac{2}{3}\gamma_{c'v'} + \left(\frac{4}{3}\ln 2 - \frac{1}{3}\right)\gamma_{c'v'}^2 + \left(S_0 - \frac{2}{15}a_{cv}^2\kappa^2\right)\gamma_{c'v'}^3 + O(\gamma_{c'v'}^4),$$

where $S_0 \approx 0.5633$, shows that $N^{(a-f)}$ is approximately 1 and nearly constant as a function of ω . The same is true of $N^{(a-a)}$, which has the expansion

$$N^{(a-a)} = 1 - \frac{2}{a_{cv}}(a_{c'v'} - a_{cv})P + O(\gamma_{c'v'}^4),$$

where, with $S_1 \approx 1.645$,

$$P \equiv \gamma_{c'v'} + \left(2\ln 2 - \frac{a_{c'v'}}{a_{cv}}\right)\gamma_{c'v'}^2 + \left(\frac{2a_{c'v'}^2}{3a_{cv}^2} - \frac{2a_{c'v'}}{a_{cv}} - \frac{1}{3}a_{c'v'}^2\kappa^2 + S_1\right)\gamma_{c'v'}^3.$$

In fact, when $\mu_{cv} = \mu_{c'v'}$, $N^{(a-a)} = 1$ even to fourth order in $\gamma_{c'v'}$. Fig. 4 shows a numerical integration of $N^{(a-f)}$ using the parameters of GaAs.

APPENDIX B: EVALUATION OF THE CURRENT INJECTION TENSOR

The tensor $\eta_{cc'vv'}^{ijkl}$, defined in (41), can be used to calculate the current injection tensor with or without excitonic effects using (38) or (44). It can be evaluated analytically in the approximation of parabolic bands. Part of the result for the 8 band Kane model has been given before but without the split-off band as an initial or intermediate state.¹³ We here give

more detail, but only for the two-band terms. We denote the bands by a double index n and s , where n is one of $\{c, hh, lh, so\}$, and s runs over the two spin states for each band. Since the Coulomb corrections to $\eta_{(I)}$ in (38) do not depend on the spin index, we can include the sum over spin indices from (38) in $\eta_{c,v,v'}^{ijkl}$. And, since we are only calculating two-band terms, we set $c' = c$ and $v' = v$. Thus

$$\begin{aligned}\eta_{ccvv}^{ijkl} &= i \frac{\pi e^4}{\hbar^2 \omega^3} \sum_{s,s'} \frac{1}{L^3} \sum_{\mathbf{k}} \Delta_{cv}^i \frac{\{(\mathbf{v}_{cc} - \mathbf{v}_{vv}), \mathbf{v}_{cs,vs'}^*\}^{jk}}{E_{cv} - \hbar \omega} v_{cs,vs'}^l \delta(2\omega - E_{cv}(k)/\hbar) \\ &= i \frac{\pi e^4}{\hbar^3 \omega^4} \frac{1}{8\pi^3} \int k^2 dk \frac{\mu_{cv}}{\hbar k_{cv}} \delta(k - k_{cv}) d\Omega \sum_{s,s'} \frac{\hbar k^i}{\mu_{cv}} \frac{1}{2} \frac{\hbar k^j}{\mu_{cv}} v_{vs',cs}^k v_{cs,vs'}^l + (j \leftrightarrow k) \\ &= i \frac{e^4}{\hbar^2 \omega^4} \frac{1}{8\pi^2} \frac{k_{cv}^3}{\mu_{cv}} \frac{1}{2} \int d\Omega \hat{k}^i \hat{k}^j \sum_{s,s'} v_{vs',cs}^k v_{cs,vs'}^l + (j \leftrightarrow k)\end{aligned}$$

where

$$k_{cv} = \sqrt{\frac{2\mu_{cv}}{\hbar^2} (2\hbar\omega - E_{cv}^g)}.$$

For $v = lh$ or hh , $E_{cv}^g = E_g$, while for $v = so$, $E_{cv}^g = E_g + \Delta$, where E_g is the fundamental band gap, and Δ is the spin-orbit splitting. The interband velocity matrix elements are approximated by their value at $k = 0$, but still depend on the direction of \mathbf{k} . In terms of the orthogonal triple of unit vectors $\hat{\mathbf{k}}$, $\hat{\mathbf{l}}$ and $\hat{\mathbf{m}}$,

$$\hat{\mathbf{k}} = \sin \theta \cos \phi \hat{\mathbf{x}} + \sin \theta \sin \phi \hat{\mathbf{y}} + \cos \theta \hat{\mathbf{z}}$$

$$\hat{\mathbf{l}} = \cos \theta \cos \phi \hat{\mathbf{x}} + \cos \theta \sin \phi \hat{\mathbf{y}} - \sin \theta \hat{\mathbf{z}}$$

$$\hat{\mathbf{m}} = -\sin \phi \hat{\mathbf{x}} + \cos \phi \hat{\mathbf{y}},$$

these matrix elements are:

$$\begin{aligned}\mathbf{v}_{c,s;hh,s'} &= \frac{1}{2} \sqrt{\frac{E_P}{m}} \left[\hat{\mathbb{I}} + i \hat{\mathbf{m}} \sigma_z \right]_{s,s'} \\ \mathbf{v}_{c,s;lh,s'} &= -\frac{1}{2} \sqrt{\frac{E_P}{3m}} \left[2\hat{\mathbf{k}} \mathbb{I} + i \hat{\mathbf{l}} \sigma_y - i \hat{\mathbf{m}} \sigma_x \right]_{s,s'} \\ \mathbf{v}_{c,s;so,s'} &= \sqrt{\frac{E_P}{6m}} \left[\hat{\mathbf{k}} \mathbb{I} - i \hat{\mathbf{l}} \sigma_y + i \hat{\mathbf{m}} \sigma_x \right]_{s,s'},\end{aligned}$$

where E_P is the Kane energy.⁹² Here, \mathbb{I} is the 2×2 identity matrix and σ_i are the Pauli spin matrices. Of course, for parabolic bands, the intraband matrix elements are $\langle n, s, \mathbf{k} | \mathbf{v} | n, s', \mathbf{k} \rangle = \delta_{s,s'} \hat{\mathbf{k}} \hbar k / m_n$, where m_n is the effective mass of band n . (In the proper Kane model, the effective masses are given in terms of the parameters E_g , Δ , and E_P , but

we treat them as additional parameters, which is equivalent to including remote band effects on the effective masses.) The sums over spin then yield

$$\begin{aligned}\sum_{s,s'} v_{hh,s';c,s}^k v_{c,s;hh,s'}^l &= \frac{E_P}{2m} (\delta_{k,l} - \hat{k}^k \hat{k}^l) \\ \sum_{s,s'} v_{lh,s';c,s}^k v_{c,s;lh,s'}^l &= \frac{E_P}{2m} \left(\hat{k}^k \hat{k}^l + \frac{1}{3} \delta_{k,l} \right) \\ \sum_{s,s'} v_{so,s';c,s}^k v_{c,s;so,s'}^l &= \frac{E_P}{3m} \delta_{k,l}.\end{aligned}$$

The remaining angular integrals can be done using

$$\begin{aligned}\int d\Omega \hat{k}^i \hat{k}^j &= \frac{4\pi}{3} \delta_{i,j} \\ \int d\Omega \hat{k}^i \hat{k}^j \hat{k}^k \hat{k}^l &= \frac{4\pi}{15} (\delta_{i,j} \delta_{k,l} + \delta_{i,k} \delta_{j,l} + \delta_{i,l} \delta_{j,k}).\end{aligned}$$

The result for $\eta_{(I\text{-free})}$ is

$$\eta_{(I\text{-free})}^{ijkl} = i \frac{\sqrt{2}}{9\pi} \frac{e^4 E_P}{\omega^4 \hbar^5 \sqrt{m}} \left[(2\hbar\omega - E_g)^{\frac{3}{2}} (T_{hh}^{ijkl} + T_{lh}^{ijkl}) + (2\hbar\omega - E_g - \Delta)^{\frac{3}{2}} T_{so}^{ijkl} \right], \quad (\text{B1})$$

where the tensor properties are

$$\begin{aligned}T_{hh}^{ijkl} &= \sqrt{\frac{\mu_{c,hh}}{m}} \left(\frac{9}{20} \delta_{i,j} \delta_{k,l} + \frac{9}{20} \delta_{i,k} \delta_{j,l} - \frac{3}{10} \delta_{i,l} \delta_{j,k} \right) \\ T_{lh}^{ijkl} &= \sqrt{\frac{\mu_{c,lh}}{m}} \left(\frac{11}{20} \delta_{i,j} \delta_{k,l} + \frac{11}{20} \delta_{i,k} \delta_{j,l} + \frac{3}{10} \delta_{i,l} \delta_{j,k} \right) \\ T_{so}^{ijkl} &= \frac{1}{2} \sqrt{\frac{\mu_{c,so}}{m}} (\delta_{i,j} \delta_{k,l} + \delta_{i,k} \delta_{j,l}),\end{aligned}$$

and the term involving T_{so}^{ijkl} should not be included if $2\hbar\omega < E_g + \Delta$. The free particle current injection tensor has also been investigated for parabolic bands, but with a simple three-band model.⁹³ That model does not have the matrix elements $\mathbf{v}_{c\uparrow, lh\downarrow}$ and $\mathbf{v}_{c\downarrow, lh\uparrow}$, and thus differs from our result for T_{lh}^{xxxx} .

ACKNOWLEDGMENTS

This work was financially supported by the Natural Science and Engineering Research Council, Photonics Research Ontario, and the US Defense Advanced Research Projects Agency. We gratefully acknowledge many stimulating discussions with Daniel Côté, James

Fraser, Ali Najmaie, Fred Nastos, Eugene Sherman, Art Smirl, Marty Stevens, and Henry van Driel.

- ¹ E. A. Manykin and A. M. Afanasev, Sov. Phys. JETP **25**, 828 (1967).
- ² M. Shapiro and P. Brumer, J. Chem. Soc. Faraday Trans. **93**, 1263 (1997).
- ³ R. J. Gordon, L. Zhu, and T. Seideman, Acc. Chem. Res. **32**, 1007 (1999).
- ⁴ Y. Y. Yin, C. Chen, D. S. Elliott, and A. V. Smith, Phys. Rev. Lett. **69**, 2353 (1992).
- ⁵ N. B. Baranova, I. M. Beterov, B. Y. Zel'dovich, I. I. Ryabtsev, A. N. Chudinov, and A. A. Shul'ginov, JETP Lett. **55**, 439 (1992).
- ⁶ B. Sheehy, B. Walker, and L. F. DiMauro, Phys. Rev. Lett. **74**, 4799 (1995).
- ⁷ E. M. Baskin and M. V. Éntin, JETP Lett. **48**, 601 (1988).
- ⁸ M. V. Éntin, Sov. Phys. Semicond. **23**, 664 (1989).
- ⁹ E. Dupont, P. B. Corkum, H. C. Liu, M. Buchanan, and Z. R. Wasilewski, Phys. Rev. Lett. **74**, 3596 (1995).
- ¹⁰ W. Pötz, Appl. Phys. Lett. **72**, 3002 (1998).
- ¹¹ R. Atanasov, A. Haché, J. L. P. Hughes, H. M. van Driel, and J. E. Sipe, Phys. Rev. Lett. **76**, 1703 (1996).
- ¹² A. Haché, Y. Kostoulas, R. Atanasov, J. L. P. Hughes, J. E. Sipe, and H. M. van Driel, Phys. Rev. Lett. **78**, 306 (1997).
- ¹³ R. D. R. Bhat and J. E. Sipe, Phys. Rev. Lett. **85**, 5432 (2000).
- ¹⁴ M. J. Stevens, A. L. Smirl, R. D. R. Bhat, J. E. Sipe, and H. M. van Driel, J. Appl. Phys. **91**, 4382 (2002).
- ¹⁵ M. J. Stevens, A. L. Smirl, R. D. R. Bhat, A. Najmaie, J. E. Sipe, and H. M. van Driel, Phys. Rev. Lett. **90**, 136603 (2003).
- ¹⁶ J. Hübner, W. W. Rühle, M. Klude, D. Hommel, R. D. R. Bhat, J. E. Sipe, and H. M. van Driel, Phys. Rev. Lett. **90**, 216601 (2003).
- ¹⁷ A. Najmaie, R. D. R. Bhat, and J. E. Sipe, Phys. Rev. B **68**, 165348 (2003).
- ¹⁸ D. H. Marti, M.-A. Dupertuis, and B. Deveaud, Phys. Rev. B **69**, 35335 (2004).
- ¹⁹ J. M. Fraser, A. I. Shkrebtii, J. E. Sipe, and H. M. van Driel, Phys. Rev. Lett. **83**, 4192 (1999).
- ²⁰ J. M. Fraser and H. M. van Driel, Phys. Rev. B **68**, 85208 (2003).

- ²¹ M. J. Stevens, R. D. R. Bhat, J. E. Sipe, H. M. van Driel, and A. L. Smirl, *phys. stat. sol. (b)* **238**, 568 (2003).
- ²² M. J. Stevens, R. D. R. Bhat, A. Najmaie, H. M. van Driel, J. E. Sipe, and A. L. Smirl, in *Optics of semiconductors and their nanostructures*, edited by H. Kalt and M. Hetterich (Springer, Berlin, 2004), vol. 146 of *Springer series in solid-state sciences*, p. 209.
- ²³ M. Shapiro, J. W. Hepburn, and P. Brumer, *Chem. Phys. Lett.* **149**, 451 (1988).
- ²⁴ M. Shapiro and P. Brumer, *Principles of the quantum control of molecular processes* (John Wiley, New York, 2003).
- ²⁵ L. Zhu, V. Kleiman, X. Li, S. P. Lu, K. Trentelman, and R. J. Gordon, *Science* **270**, 77 (1995).
- ²⁶ T. Seideman, *J. Chem. Phys.* **108**, 1915 (1998).
- ²⁷ T. Seideman, *J. Chem. Phys.* **111**, 9168 (1999).
- ²⁸ N. B. Baranova, A. N. Chudinov, and B. Y. Zel'dovich, *Opt. Comm.* **79**, 116 (1990).
- ²⁹ V. A. Pazdzersky and V. I. Usachenko, *J. Phys. B: At. Mol. Opt. Phys.* **30**, 3387 (1997).
- ³⁰ H. Haug and S. W. Koch, *Quantum theory of the optical and electronic properties of semiconductors* (World Scientific, Singapore, 1993).
- ³¹ S. Albrecht, L. Reining, R. D. Sole, and G. Onida, *Phys. Rev. Lett.* **80**, 4510 (1998).
- ³² L. X. Benedict, E. L. Shirley, and R. B. Bohn, *Phys. Rev. Lett.* **80**, 4514 (1998).
- ³³ L. X. Benedict, E. L. Shirley, and R. B. Bohn, *Phys. Rev. B* **57**, R9385 (1998).
- ³⁴ M. Rohlfing and S. G. Louie, *Phys. Rev. Lett.* **81**, 2312 (1998).
- ³⁵ M. Rohlfing and S. G. Louie, *Phys. Rev. B* **62**, 4927 (2000).
- ³⁶ R. J. Elliott, *Phys. Rev.* **108**, 1384 (1957).
- ³⁷ R. Loudon, *Proc. Phys. Soc.* **80**, 952 (1962).
- ³⁸ G. D. Mahan, *Phys. Rev.* **170**, 825 (1968).
- ³⁹ K. C. Rustagi, F. Pradere, and A. Mysyrowicz, *Phys. Rev. B* **8**, 2721 (1973).
- ⁴⁰ C. C. Lee and H. Y. Fan, *Phys. Rev. B* **9**, 3502 (1974).
- ⁴¹ E. Doni, G. P. Parravicini, and R. Girlanda, *Solid State Commun.* **14**, 873 (1974).
- ⁴² M. Sondergeld, *phys. stat. sol. (b)* **81**, 451 (1977).
- ⁴³ R. Girlanda, A. Quattropani, and P. Schwendimann, *Phys. Rev. B* **24**, 2009 (1981).
- ⁴⁴ D. F. Blossey, *Phys. Rev. B* **2**, 3976 (1970).
- ⁴⁵ A. K. Ganguly and J. L. Birman, *Phys. Rev.* **162**, 806 (1967).
- ⁴⁶ R. M. Martin, *Phys. Rev. B* **4**, 3676 (1971).

- ⁴⁷ A. García-Cristóbal, A. Cantarero, C. Trallero-Giner, and M. Cardona, Phys. Rev. B **49**, 13430 (1994).
- ⁴⁸ A. García-Cristóbal, A. Cantarero, C. Trallero-Giner, and M. Cardona, Phys. Rev. B **58**, 10443 (1998).
- ⁴⁹ M. A. Kolber and J. D. Dow, Phys. Rev. B **18**, 5499 (1978).
- ⁵⁰ M. Sheik-Bahae, J. Wang, and E. W. V. Stryland, IEEE J. Quantum Electron. **30**, 249 (1994).
- ⁵¹ E. K. Chang, E. L. Shirley, and Z. H. Levine, Phys. Rev. B **65**, 35205 (2002).
- ⁵² D. W. Schumacher and P. H. Bucksbaum, Phys. Rev. A **54**, 4271 (1996).
- ⁵³ P. A. Roos, Q. Quraishi, S. T. Cundiff, R. D. R. Bhat, and J. E. Sipe, Optics Express **11**, 2081 (2003).
- ⁵⁴ T. M. Fortier, P. A. Roos, D. J. Jones, S. T. Cundiff, R. D. R. Bhat, and J. E. Sipe, Phys. Rev. Lett. **92**, 147403 (2004).
- ⁵⁵ P. A. Roos, X. Li, J. A. Pipis, S. T. Cundiff, R. D. R. Bhat, and J. E. Sipe, J. Opt. Soc. Am. B **22**, 362 (2005).
- ⁵⁶ A. Haché, J. E. Sipe, and H. M. van Driel, IEEE J. Quantum Electron. **34**, 1144 (1998).
- ⁵⁷ D. Côté, J. M. Fraser, M. DeCamp, P. H. Bucksbaum, and H. M. van Driel, Appl. Phys. Lett. **75**, 3959 (1999).
- ⁵⁸ P. Král and J. E. Sipe, Phys. Rev. B **61**, 5381 (2000).
- ⁵⁹ V. I. Shelest and M. V. Éntin, Sov. Phys. Semicond. **13**, 1353 (1979).
- ⁶⁰ V. I. Belinicher and B. I. Sturman, Sov. Phys. Usp. **23**, 199 (1980).
- ⁶¹ C. Aversa and J. E. Sipe, IEEE J. Quant. Electron. **32**, 1570 (1996).
- ⁶² B. I. Sturman and V. M. Fridkin, *The photovoltaic and photorefractive effects in noncentrosymmetric materials* (Gordon and Breach, Philadelphia, 1992).
- ⁶³ J. E. Sipe and A. I. Shkrebtii, Phys. Rev. B **61**, 5337 (2000).
- ⁶⁴ D. Côté, N. Laman, and H. M. van Driel, Appl. Phys. Lett. **80**, 905 (2002).
- ⁶⁵ J. O. Dimmock (Academic Press, New York, 1967), vol. 3 of *Semiconductors and semimetals*, chap. 7, p. 259.
- ⁶⁶ V. Nathan, A. H. Guenther, and S. S. Mitra, J. Opt. Soc. Am. B **2**, 294 (1985).
- ⁶⁷ P. Y. Yu and M. Cardona, *Fundamentals of Semiconductors* (Springer, Berlin, 1996), chap. 6.
- ⁶⁸ F. Bassani and G. P. Parravicini, *Electronic states and optical transitions in solids* (Pergamon Press, Oxford, 1975), chap. 6.

- ⁶⁹ C. Aversa and J. E. Sipe, Phys. Rev. B **52**, 14636 (1995).
- ⁷⁰ A. Baldereschi and N. O. Lipari, Phys. Rev. B **3**, 439 (1971).
- ⁷¹ G. Breit and H. A. Bethe, Phys. Rev. **93**, 888 (1954).
- ⁷² J. R. Taylor, *Scattering Theory* (John Wiley & Sons, New York, 1972).
- ⁷³ This follows from the relation between ionization and scattering states, and the scattering states given in, e.g., Ref.74.
- ⁷⁴ L. I. Schiff, *Quantum Mechanics* (McGraw-Hill, New York, 1955), p. 119, 2nd ed.
- ⁷⁵ J. M. Luttinger and W. Kohn, Phys. Rev. **97**, 869 (1955).
- ⁷⁶ G. Dresselhaus, J. Phys. Chem. Solids **1**, 14 (1956).
- ⁷⁷ M. Sondergeld, phys. stat. sol. (b) **81**, 253 (1977).
- ⁷⁸ A. Baldereschi and N. O. Lipari, Phys. Rev. B **8**, 2697 (1973).
- ⁷⁹ A. Baldereschi and N. O. Lipari, Phys. Rev. Lett. **25**, 373 (1970).
- ⁸⁰ R. D. R. Bhat and J. E. Sipe (2004), unpublished.
- ⁸¹ G. L. Bir and G. E. Pikus, *Symmetry and strain-induced effects in semiconductors* (Keter, Jerusalem, 1974), English ed., Eq. 17.33.
- ⁸² H. A. Bethe and E. E. Salpeter, *Quantum mechanics of one- and two-electron atoms* (Plenum, New York, 1977).
- ⁸³ O. Madelung, ed., *Semiconductors - Basic Data* (Springer-Verlag, Berlin, 1996), 2nd ed.
- ⁸⁴ P. Pfeffer and W. Zawadzki, Phys. Rev. B **41**, 1561 (1990).
- ⁸⁵ D. D. Sell, Phys. Rev. B **6**, 3750 (1972).
- ⁸⁶ M. D. Sturge, Phys. Rev. **127**, 768 (1962).
- ⁸⁷ M. H. Weiler, Solid State Commun. **39**, 937 (1981).
- ⁸⁸ J. P. van der Ziel, Phys. Rev. B **16**, 2775 (1977).
- ⁸⁹ J. E. Sipe, A. I. Shkrebtii, and O. Pulci, phys. stat. sol. (a) **170**, 431 (1998).
- ⁹⁰ At higher excitation densities, the Coulomb interaction can modify the maximum spin separation distance through the momentum relaxation time.
- ⁹¹ Mahan instead defines a quantity $J_{\kappa} = N(\kappa)\gamma^2 \left(1 + (a\gamma\kappa)^2\right)^{-1}$.³⁸
- ⁹² E. O. Kane, J. Phys. Chem. Solids **1**, 249 (1957).
- ⁹³ M. Sheik-Bahae, Phys. Rev. B **60**, R11257 (1999).